Available online at www.sciencedirect.com
SCIENCE DIRECT®
ELSEVIER
Journal of Magnetism and Magnetic Materials 283 (2004) 133–142
Journal of magnetism and magnetic materials
www.elsevier.com/locate/jmmm

Magnetic configurations in anisotropic stripe systems

F. Porrati[a,*], H.P. Oepen[b], J. Kirschner[a]

[a] *Max-Planck-Institut für Mikrostrukturphysik, Weinberg 2, D-06120 Halle, Germany*
[b] *Institut für Angewandte Physik, Jungiusstr. 11, D-20355 Hamburg, Germany*

Received 31 March 2004; received in revised form 10 May 2004
Available online 15 June 2004

Abstract

Numerical micromagnetic simulations are performed to study the magnetic configurations of ultrathin films with spatially varying magnetic anisotropy. Investigating infinitely long stripes with alternating in-plane/out-of-plane uniaxial anisotropy we find states of uniform, canted and alternating magnetization as function of the width of the stripes. A simple analytical model is given to describe the canting by means of a fourth order anisotropy term that is caused solely by the microstructure. Furthermore, the system is described macroscopically by averaging the magnetization of the various states. In this framework the spin reorientation transition between states of uniform magnetization is studied as a function of the stripes density. We find that the rotation of the average magnetization takes place always continuously and is sharper for a higher density of stripes.

PACS: 75.70.Ak; 75.30.Gw; 75.70.Kw

Keywords: Magnetic anisotropy; Ultrathin films; Spin reorientation transition

1. Introduction

The interest for magnetic materials of reduced dimensionality is growing continuously in fundamental and applied research. The ability to control the magnetic properties of materials at the nanometer scale is leading to smaller and faster magneto-electronic devices [1]. Among the possibilities offered by spin engineering, the patterning of continuous magnetic media is of major interest for the potential application in magneto-recording industry. Indeed, such media offer the advantage to control the spin configuration as well as to overcome bit-size limitations due to superparamagnetism and reduced Curie temperature present in granular media and quantum dot arrays [2]. Experimentally the local tailoring of the magnetic anisotropy has been obtained by ion irradiation [3]

*Corresponding author. Physikalisches Institut Frankfurt University, Thin Films, Robert-Mayer Str. 2-4, Frankfurt am Main 60054, Germany. Tel.: +49-6979822132; fax: +49-6979822348
E-mail address: porrati@physik.uni-frankfurt.de (F. Porrati).

0304-8853/$ - see front matter © 2004 Elsevier B.V. All rights reserved.
doi:10.1016/j.jmmm.2004.05.014

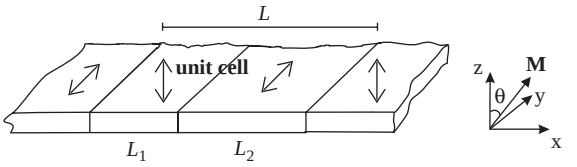

Fig. 1. Series of infinitely long stripes with alternating uniaxial anisotropies. The arrows indicate the axes of easy magnetization.

and by selective epitaxial growth [4]. Thus artificially confined magnetic domains are built on a scale determined by the local patterning. In theory the response of the fine magnetic structure, i.e., magnetic domains, domain walls, etc., to the lateral confinement can be investigated by means of micromagnetics.

In this paper, we model planar patterned magnetic media in the limit of ultrathin films by considering a series of infinitely long stripes with alternating in-plane/out-of-plane magnetization easy axis (see Fig. 1). We investigate the magnetic configuration as a function of two parameters: the period of the structure (L), i.e., the sum of the widths of two neighboring stripes, and the ratio between the width of one stripe and L. In the first part of the paper a detailed microscopic analysis of the magnetic states is performed. In the second part the investigation is generalized by considering the average magnetization. Finally, the results of the investigation are discussed and briefly summarized.

2. Modelling

The system studied is sketched in Fig. 1. The unit cell is given by two stripes of width L_1 and L_2 infinitely long in the y direction. The magnetization easy axis in neighboring stripes changes periodically between out-of-plane and in-plane. Periodical boundary conditions are imposed in the x direction and in the y direction, the latter to simulate the infinity of the stripes. The orientation of the magnetization vector **M** can vary with the x position while it is not depending on the y and z position. The magnetic configuration of the system is obtained numerically [5] by solving iteratively the Landau–Lifshiz–Gilbert equation [6] related to the problem.

2.1. Magnetic configurations

In this section, we study the magnetic configurations in anisotropic stripe systems by fixing the width of the unit cell L and varying the ratio L_1/L. The stripes of width L_1 have perpendicular easy axis. The analysis is on the microscopic scale, i.e., the micromagnetic structure of the system is analyzed by plotting the spatial variation of the angle θ, defined as the angle between the magnetization **M** and the normal **n** to the surface of the film. In order to calculate the magnetization profiles we use the values of the anisotropy constants for the system Pd/Co/Pd(1 1 1) deduced from experiments [7]. This choice does not influence the generality of our study since similar magnetic configurations can be obtained by using other values of the anisotropy constants. From the experiment it is known that 4 ML of Co/Pd(1 1 1) have in-plane easy axis. By covering the film with an overlayer of Pd the direction of the easy axis reorients out-of-plane. The resulting second-order effective anisotropy constants[1] for the uncovered and for the covered system are $k_{\mathrm{Co}}^{\mathrm{eff}} = -k_{\mathrm{Pd}}^{\mathrm{eff}} = -0.48 \times 10^7\ \mathrm{erg/cm^3}$. In our numerical investigation we use these constants for the system of stripes with alternating uniaxial anisotropies. Higher order anisotropy terms are neglected. The values of bulk Co are used for the saturation magnetization ($M_{\mathrm{s}} = 1440\ \mathrm{emu/cm^3}$) and the exchange stiffness constant ($A_{\mathrm{ex}} = 1.55 \times 10^{-6}\ \mathrm{erg/cm}$). The simulation volume is divided in cubes of 1 nm size.

In Fig. 2 we plot the magnetization profiles calculated numerically as a function of L_1/L. The simulation is performed by choosing as a starting condition a state of uniform magnetization canted at 45° with respect to the normal. The magnetization components are $M_y = M_z = 0.707$ and $M_x = 0$. Note that the same magnetization

[1] The effective anisotropy k^{eff} is defined as the difference between the uniaxial anisotropy k_{u} (result of surface and bulk contributions) and $2\pi M_{\mathrm{s}}^2$ the magnetostatic energy of an infinite film uniformly magnetized out-of-plane.

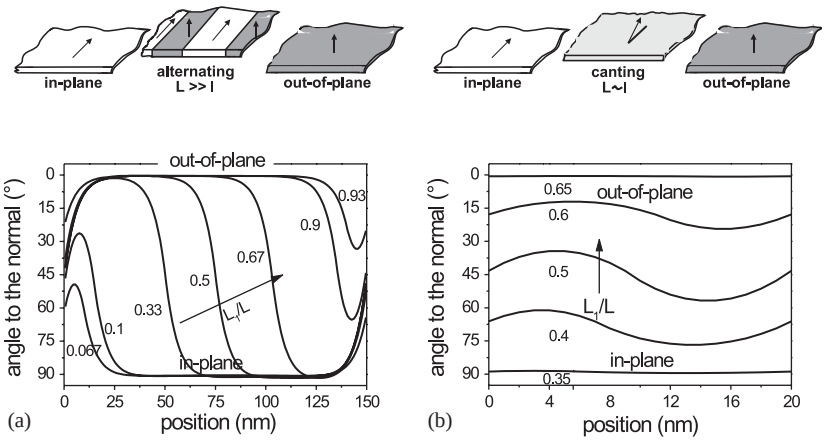

Fig. 2. Micromagnetic configurations obtained for a unit cell L much larger than the magnetic characteristic length λ (a) and for $L \sim \lambda$ (b). In each figure the magnetization profiles are plotted for various values of the ratio L_1/L.

configurations are obtained for any other angle of canting as starting parameter. In Fig. 2(a) we plot the result of the simulation for the system of stripes with unit cell $L = 150$ nm. In this case the unit cell is much wider than the magnetic characteristic length, i.e., $L \gg \lambda$, with $\lambda = \sqrt{A_{ex}/k} = 5.68$ nm. For $L_1/L = 0.067$ ($L_1 \simeq 10$ nm) the magnetization is mainly in-plane. Only a small out-of-plane contribution due to the out-of-plane anisotropy is present. Such a contribution is localized around the center of the stripe of width L_1. The localization around the center of the stripe is due to the periodical boundary conditions used for the simulations. The problem to find the onset for perpendicular (or parallel) magnetization for films with laterally modulated anisotropies was solved analytically by Elmers [8]. From the calculation one can deduce that the onset is at $L_1/\lambda = \pi/2$. As a consequence $L_1 \simeq 8.9$ nm, for $\lambda = 5.68$ nm. In our case we find $6 \leqslant L_1 \leqslant 10.5$ nm for $0.04 \leqslant L_1/L \leqslant 0.07$ as one can deduce from Fig. 8(a). Thus our result is in agreement with the calculation of Ref. [8]. For $L_1/L = 0.33$ the out-of-plane component of the magnetization is fully evolved in L_1 and the magnetization changes from complete in-plane to out-of-plane alignment. For $L_1/L > 0.5$ the out-of-plane component is dominating in the larger part of the structure. For $L_1/L = 0.93$ the system is magnetized almost completely out-of-plane. A small in-plane contribution is still present localized around the center of the stripe with in-plane anisotropy. The micromagnetic picture changes completely for $L = 20$ nm. In this case the width of the unit cell is of the same order as the magnetic characteristic length. In Fig. 2(b) we plot the corresponding magnetization profiles. For $L_1/L = 0.35$ the magnetization slightly oscillates around $\theta \simeq 87^\circ$. The amplitude of the oscillation increases with L_1/L becoming maximum for $\theta = 45^\circ$. For $L_1/L > 0.5$ the amplitude gradually decreases until the magnetization is uniformly out-of-plane. Note that in experiments these oscillations might be detected with the help of magnetic imaging techniques [9] with the appropriate spatial resolution.

2.2. Higher-order anisotropy

The possibility to obtain states of canted magnetization due to inhomogeneities of the magnetic anisotropy in the vertical direction of the film has been addressed in the past [10–12]. Alternative states of canting can be obtained for films with lateral inhomogeneities. The role of higher-order anisotropy terms in films with spatial fluctuations of the second-order anisotropy was investigated in the limit of small angular oscillations of the magnetization direction [13]. In those papers an elegant mathematical analysis was

carried out following the study of Slonczewski for biquadratic exchange coupled multilayers [14]. The authors found that the spatial fluctuation of the anisotropy gives rise to a canted state phenomenologically described by a higher-order anisotropy term which is the minimum when the average magnetization lies at 45° with respect to the normal of the film. In the following we resume these results by comparing numerical micromagnetic calculations with a simple phenomenological model. Although the modeling neglects the mathematical details contained in the previous studies, it gives a clear insight into the physics of the problem and leads to the same qualitative results as Ref. [13]. The goal of this section is to describe systems with alternating anisotropies for a width of the unit cell comparable to the magnetic characteristic length, i.e., $L \sim \lambda$. With respect to Fig. 1 we write the total energy density of the unit cell by means of second-order anisotropy constants

$$f(\theta) = k_{\mathrm{sh}} + k_{\mathrm{tot}} \sin^2 \theta, \tag{1}$$

where $k_{\mathrm{tot}} = k_1^{\mathrm{eff}} L_1/L + k_2^{\mathrm{eff}} L_2/L = A + B$, $k_1^{\mathrm{eff}} = k_1 - k_{\mathrm{sh}}$, $k_2^{\mathrm{eff}} = k_2 - k_{\mathrm{sh}}$ and $k_{\mathrm{sh}} = 2\pi M_s^2$. Eq. (1) is valid in the limit of uniformly magnetized films. The anisotropy constant k_{tot} is the sum of the effective anisotropy constants k_1^{eff} and k_2^{eff}, weighed by the respective stripe width. The sign of k_{tot} determines which of the two contributions is dominant and the direction of the easy axis of the system. In particular the easy axis is in-plane for $k_{\mathrm{tot}} < 0$ and out-of-plane for $k_{\mathrm{tot}} > 0$. The solid line in Fig. 3(a) gives the total energy calculated by means of Eq. (1). We consider a system with unit cell $L = 5$ nm consisting of Pd stripes covering a Co/Pd(1 1 1) film. The effective anisotropy constants are assumed to be $k_{\mathrm{Pd}}^{\mathrm{eff}} = 0.6571 \times 10^7$ erg/cm^3 and $k_{\mathrm{Co}}^{\mathrm{eff}} = -0.4429 \times 10^7$ erg/cm^3, taken from Ref. [7] for the system Pd/Co/Pd(1 1 1) with a thickness of the Co film equal to 3 ML (note the difference in Co thickness compared to the previous section). For $L_1/L = 0$ and $L_1/L = 0.2$ ($k_{\mathrm{tot}} < 0$) the system shows an in-plane easy axis. For $L_1/L = 0.6$, $L_1/L = 0.8$ and $L_1/L = 1$ ($k_{\mathrm{tot}} > 0$) the direction of the easy axis reorients out-of-plane. The transition takes place for $L_1/L = 0.4$ ($k_{\mathrm{tot}} = 0$) where no angular variation

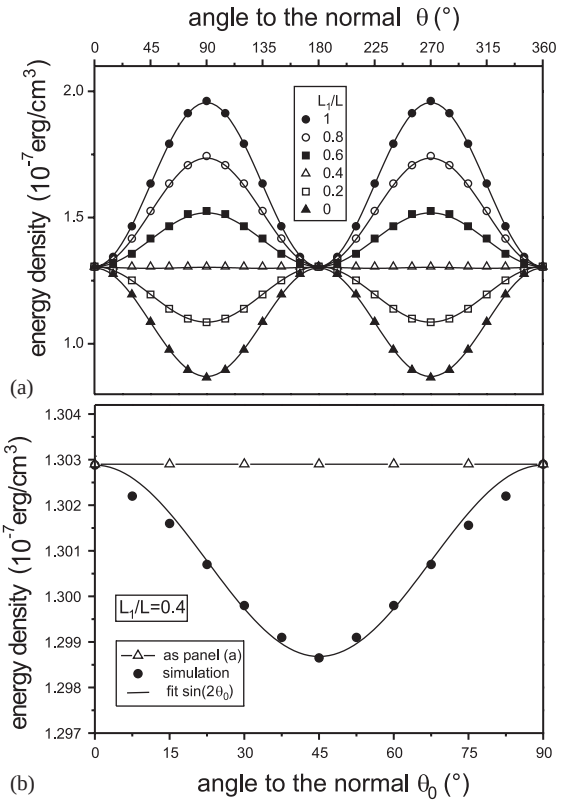

Fig. 3. Panel (a) Total energy density vs. angle to the normal for various values of the ratio L_1/L. Solid lines: analytical description following Eq. (1). Symbols: numerical values. Panel (b) After relaxation, the system for $L_1/L = 0.4$ shows a minimum of the energy for $\theta_0 = 45°$ (Pd/Co/Pd(1 1 1) film, with 3 ML Co). The black points were obtained during the relaxation process that brings the system from the starting condition (uniform in-plane or out-of-plane magnetization) to the minimum.

of the energy is expected from Eq. (1). In Fig. 3(a) we compare the results of Eq. (1) with the energies obtained from the simulation when assuming a uniform magnetization with constant angle θ. Such configuration was then used as starting condition for the simulation, which yields the state of lowest energy. As expected, for $L_1/L = 0$ and $L_1/L = 0.2$ the system relaxes to a state with in-plane uniform magnetization; for $L_1/L = 0.6$, $L_1/L = 0.8$ and $L_1/L = 1$, the minimum is a state with uniform magnetization directed out-of-plane. The most interesting magnetic structure is

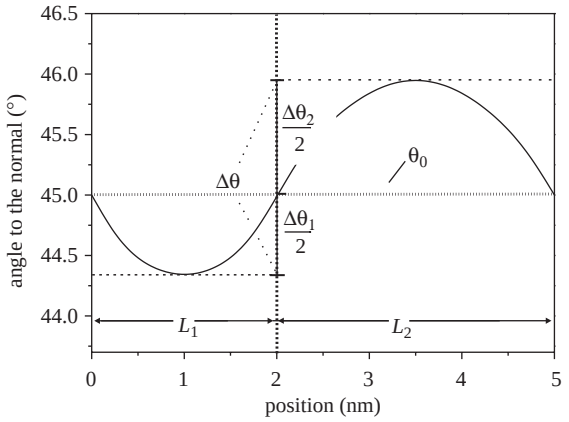

Fig. 4. Magnetization profile obtained for $L = 5$ nm. The magnetization direction slightly oscillates around $\theta_0 = 45°$.

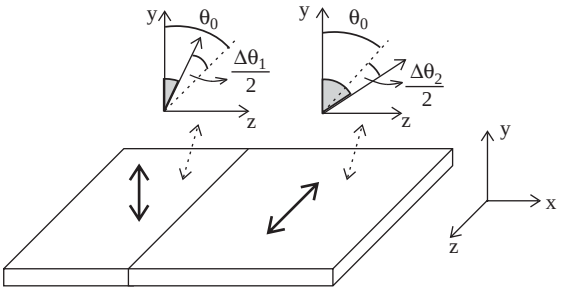

Fig. 5. Modeling in the limit of $L \sim \lambda$, see text.

obtained for $L_1/L = 0.4$ ($k_{tot} = 0$). In this case the shape of the magnetization profile results in a state of non-uniform magnetization slightly oscillating around $\theta_0 = 45°$, as shown in Fig. 4. Hence, the angular-dependent energy has a minimum at $\theta_0 = 45°$, being θ_0 the angle to the normal at the boundary of two successive stripes (see Fig. 3(b)).

In order to understand this result we extend the model represented by Eq. (1) to systems with non-uniform magnetization in the limit of $\lambda \sim L$. We call $\Delta\theta$ the deviation of the angles to the orientation of the magnetization at the center of two successive stripes. Since $\Delta\theta \ll \theta_0$ we consider the magnetization as constant inside each stripe and the system as described by means of two *macromagnetic moments* each belonging to one stripe, see Fig. 5. In the stripe with out-of-plane anisotropy the macro magnetic moment rotates in the direction towards the normal by the amount $\Delta\theta_1/2$. In the stripe with in-plane anisotropy it rotates in the opposite direction by $\Delta\theta_2/2$. In general these angles are different because the effective anisotropies are not equal. The angular dependence of the energy can be written as

$$f(\theta_0) = k_{sh} + A\sin^2\left(\theta_0 - \frac{\Delta\theta_1}{2}\right) + B\sin^2\left(\theta_0 + \frac{\Delta\theta_2}{2}\right). \quad (2)$$

Note that in the modeling the exchange energy increases with the split angle, while the anisotropy energy decreases[2]. In the limit of small splitting, i.e., $\Delta\theta_1$, $\Delta\theta_2 \approx 0$, Eq. (2) becomes

$$f(\theta_0) \approx k_{sh} + (A + B)\sin^2\theta_0 + \frac{B - A}{2}\Delta\theta\,\sin(2\theta_0) \quad (3)$$

with $\Delta\theta = \Delta\theta_1/2 + \Delta\theta_2/2$. Eq. (3) reduces to Eq. (1) if $\Delta\theta$ is zero. On the other hand, the second-order anisotropy vanishes for $A = -B$, i.e., when the weighed effective anisotropies are balanced. In this case Eq. (3) reduces to

$$f(\theta_0) \approx k_{sh} - A\,\Delta\theta\,\sin(2\theta_0). \quad (4)$$

This higher-order anisotropy term has a minimum at 45° with respect the normal in agreement with the numerical calculation of Fig. 3(b). The angle $\Delta\theta$, which determines the depth of the minimum in Fig. 3(b), is plotted in Fig. 6 as a function of θ_0 and fitted with a $\sin(2\theta_0)$ function. The maximum, that we label with c, is obtained for $\theta_0 = 45°$ and is a function of the width of the unit cell and the exchange stiffness constant. The higher-order anisotropy term is a four-fold anisotropy term with minima for $\theta_0 = 135°, 225°, 315°$ and 45°. The angle $\Delta\theta$ is positive in the first and third quadrants of the plane yz and negative in the second and fourth quadrants, i.e., $\Delta\theta \sim \pm c\,\sin(2\theta_0)$. By inserting this expression in Eq. (4) we obtain

$$f(\theta_0) \approx k_{sh} - Ac\sin^2(2\theta_0). \quad (5)$$

[2]A more correct expression of the total energy should contain also the Heisemberg exchange term $J\cos(\Delta\theta)$. However, since this term contributes only with a constant for $\Delta\theta \approx 0$, it has been omitted.

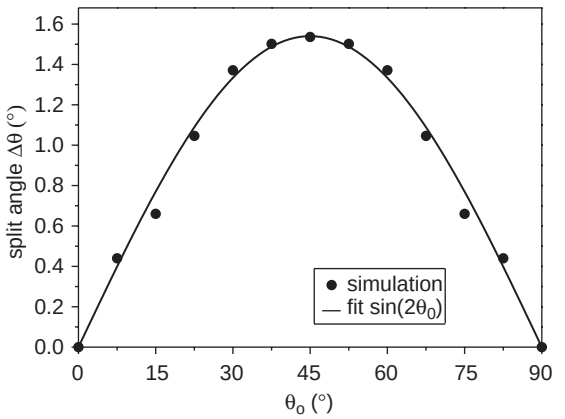

Fig. 6. Split angle $\Delta\theta$ between the magnetization direction at the center of successive stripes vs. θ_0, magnetization direction between the stripes, see Fig.4.

The minimum of the total energy obtained for $\theta_0 = 45^\circ$ with respect to the normal is explained with the help of the two macromagnetic moments. In fact, the exchange energy is a function of their split angle $\Delta\theta$ but it does not depend on their spatial orientation. On the contrary the anisotropy energy is a function of θ_0 and thus it determines the angular dependence of the total energy. In particular the gain in anisotropy energy due to the splitting is a maximum for $\theta_0 = 45^\circ$, which follows from the slope of the sin in Eq. (2). Note that in the modeling the dipolar energy is considered as a local demagnetizing energy and is part of the anisotropy energy. The correction due to the non-uniformity of the magnetization is neglected. This assumption is the more justified the smaller the modulation of the magnetization around θ_0 is, i.e. for smaller width of the unit cell [15].

2.3. Macroscopic analysis and SRT

Micromagnetics gives the most complete picture of the metastable states of a certain system. However, useful information can be obtained also by simple macroscopic considerations [16]. In the following we generalize the previous analysis by using the average projection of the normalized magnetization along the plane and the normal to the film, labelled by $m_\parallel$ and $m_\perp$, respectively. The assumed anisotropy constants are the same as Section 2.1. This analysis might help to interpret experimental results obtained by means of spatially averaging techniques [17].

If the sum of the squares of the projections is equal to one, i.e., $m_\perp^2 + m_\parallel^2 = 1$, the magnetization is uniform. As plotted in Fig. 7(a) this happens for $L = 150$ nm, if $L_1/L < 0.05$ or $L_1/L > 0.95$, and for $L = 20$ nm, if $L_1/L < 0.35$ or $L_1/L > 0.65$ (Fig. 7(b)). For $L = 150$ nm, if $L_1/L > 0.05$ the sum of the squares of the projections decreases until it reaches the minimum for $L_1/L = 0.5$. This behavior indicates the formation of magnetic domains with alternating in-plane and out-of-plane magnetization (see sketch in Fig. 7(a)). The sum of the projections (non-squared) is larger than one for $0.05 < L_1/L < 0.95$ indicating the presence of walls between successive magnetic domains. For $L = 20$ nm, if $L_1/L > 0.05$ the sum of the projections increases until it reaches the maximum for $L_1/L = 0.5$. This behavior might be erroneously attributed to states of uniform canted magnetization (sketch in Fig. 7(b)). Actually, the plot of Fig. 7(b) gives the macroscopic picture of states with oscillating magnetization (see Fig. 2(b)) rather than of states of uniform magnetization. This can be hardly recognized by the macroscopic investigation. However, the plot of Fig. 7(b) shows that the sum of the squares of the projections is slightly smaller than one for $0.35 < L_1/L < 0.65$, as expected for states of non-uniform magnetization.

It is well known that the magnetization direction can undergo a 90° rotation by changing the thickness, the temperature or the composition of the film. This phenomenon, known as spin reorientation transition (SRT), has been investigated for a variety of systems in theory and experiments. Many research groups have found that the SRT takes place either by a smooth continuous rotation of the magnetization or abruptly. As shown in Fig. 2 anisotropic stripe systems undergo a SRT by changing the ratio L_1/L. In the following we analyze the macroscopic behavior of the system during the SRT. Fig. 8(a)–(c) give the results of the simulations for three different values of the unit cell. In each panel we plot the average projections $m_\parallel$ and $m_\perp$. We define the transition interval of the SRT as the

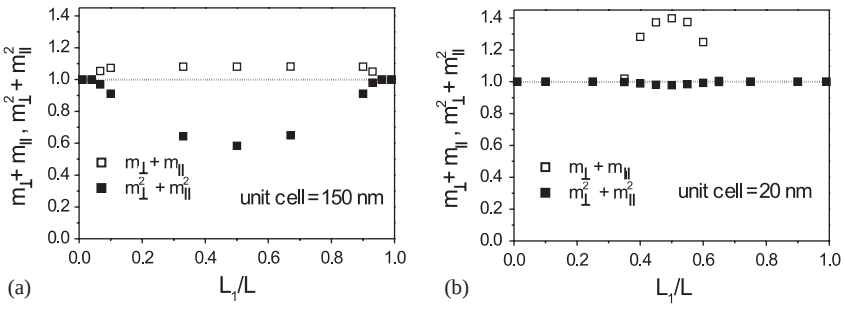

Fig. 7. Macroscopic analysis of the magnetic states. In the plots $m_\parallel$ and $m_\perp$ give the averaged projections of the magnetization of one unit cell. For simplicity the magnetization per cell is set to unity. Panel (a) shows the situation in case of a large unit cell with fully evolved laterally separated in-plane and out-of-plane magnetization orientation. In (b) the small unit cell situation is displayed. The plots show the sum $m_\parallel + m_\perp$ and the sum of the squares of the projections $m_\parallel^2 + m_\perp^2$. In (a) one should expect $m_\parallel + m_\perp = 1$, because of the magnetization rotation between the stripes with out-of-plane and in-plane magnetization orientation the calculated value is slightly higher than 1. In (b), the case of magnetization canting, one can expect $m_\parallel^2 + m_\perp^2 = 1$. The slight angle deviations (see text) cause a value smaller than 1 in the plot.

interval $\Delta L_1/L$ necessary to reorient the magnetization from uniform in-plane to uniform out-of-plane (or vice versa). The main result of the simulation is that the reorientation transition is always continuous and the transition interval decreases with the width of unit cell, see Fig. 8(d). For $L = 150$ nm (Fig. 8(a)), the transition interval covers almost the whole range available. The onset of perpendicular magnetization takes place for $L_1/L \simeq 0.05$. The weight of the in-plane and the out-of-plane projections of the magnetization is the same for $L_1/L \simeq 0.5$. For $L_1/L > 0.5$ the out-of-plane component dominates and increases with L_1/L until saturation. The value of the two components for $L_1/L \simeq 0.5$ is $m_\parallel = m_\perp = 0.5$, indicating a state with alternating in-plane and out-of-plane magnetization. For $L = 20$ nm, see Fig. 8(b), the reorientation transition takes place over half of the range available, i.e., $0.3 \leqslant L_1/L \leqslant 0.7$. In particular for $L_1/L = 0.5$ we find $m_\parallel = m_\perp \simeq 0.7$ that indicates a canting of the magnetization at 45° with respect to the normal. For $L = 4$ nm (Fig. 8(c)) the transition interval further reduces.[3]

[3]To investigate the SRT for $L = 4$ nm we use square prism with size of 1 nm in the z direction and smaller sizes in the x–y directions. The size of the square is varied between 0.138 and 0.364 nm. This choice is necessary to map narrow transition intervals.

3. Discussion

In the literature many systems are reported that reorient by means of a continuous transition of the average magnetization. For example higher-order contributions to the magnetocrystalline anisotropy [18] or magnetic domains [19] can show up at the point of compensation between shape and surface anisotropies leading to continuous spin reorientation transitions. Our investigation for ultrathin films with spatially varying magnetic anisotropies shows that the behavior of the system in the regime of the spin reorientation transition has to be attributed to both the intrinsic properties of the material and the microstructure.

The different scenarios of spin reorientation transition described in the former sections are closely related to the magnetic configurations found as a function of the length scales of the system. The average magnetization rotates from in-plane to out-of-plane by increasing the ratio L_1/L. For $L \gg \lambda$ the spin reorientation transition involves states of alternating uniform magnetization separated by a transition region where the magnetization rotates by 90°. The transition regions are determined by the interplay of the exchange and anisotropy energy. The latter changes abruptly within the transition region causing the rotation. Thus the average magnetization is simply determined by the widths of the

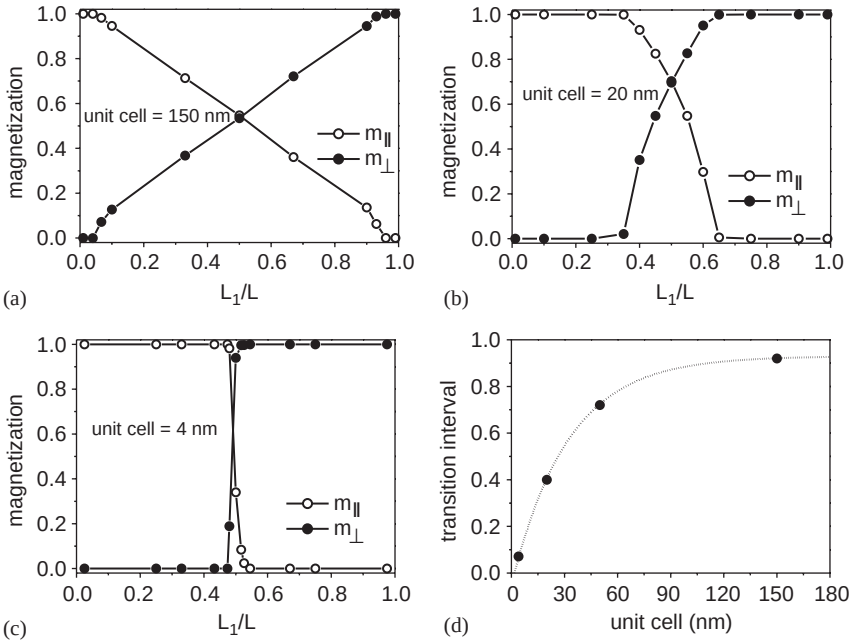

Fig. 8. Spin reorientation transition driven by the increase of the ratio L_1/L as a function of the width of the unit cell (a)–(c). Panel (d) transition interval vs. width of the unit cell.

in-plane and the out-of-plane regions. Since the average magnetization is proportional to the ratio L_1/L, the continuous change of L_1/L leads to a continuous spin reorientation transition. For $L \sim \lambda$ the magnetization is modulated periodically with an amplitude that is a function of the width of the unit cell. Magnetic domains are no more present and the reorientation transition is determined by the small variations of the magnetic wall fine structure. The spin reorientation transition is continuous since the exchange stiffness constant A_{ex} has a finite value. In fact, for an infinite value of A_{ex} the reorientation is abrupt, as shown by Eq. (1). For $A_{ex} = 0$ the average magnetization will show a linear dependence on L_1/L, like for $L \gg \lambda$, in contrast to Fig. 8(b). It is important to underline that even though the magnetic anisotropy changes abruptly from one stripe to another the behavior of the average magnetization in the regime of the spin reorientation transition is continuous on macroscopic scale and an higher-order anisotropy due to the microstructure appears. The state of canted magnetization appears at the compensation of the effective anisotropies ($k_{tot} = 0$), although intrinsic higher order anisotropy terms have not been considered in our simulations and in the analytical model. Experimentally their presence could be distinguished by changing the width of the unit cell, since the fourth-order anisotropy due to the microstructure is a function of L. In particular the depth of the energy minimum in Fig. 3(b) decreases with L as shown analytically [15]. Tuning the hardness of the material is possible via patterning. A fundamental question arises: does the system become perfectly soft at some point [20]? A number of experiments and theoretical investigations have been performed in the past on various systems in order to answer this question [21]. Our analysis shows that in thin films with spatially varying magnetic anisotropies the fourth-order magnetic anisotropy decreases with L but never vanishes for $L \neq 0$.

Usually the canting of the magnetization in ultrathin films is described by considering a fourth-order term in the expression of the anisotropy energy density [22]. Although this approach is quite general and it has been used to describe a

large number of systems, it does not give the insight into the physics of the problem. Systems with non-uniform anisotropy may be described in the framework of the phenomenological model of Ref. [22], valid for uniformly magnetized films. In this case the modulation of the magnetization is neglected and a fourth order term is introduced ad hoc to describe the reorientation of the easy axis. As soon as the width of the unit cell increases, the modulation cannot be neglected anymore and the model for uniformly magnetized films is no more strictly suitable. On the macroscopic scale the system will show two stable magnetization orientation, i.e. apparently local minima in the free energy for in-plane as well as for out-of-plane magnetization orientation, which is in literature phenomenologically explained as a state of coexisting phases [22]. On the other hand, by means of continuum [12] or discrete [10,11] modelling, the origin of the canting can explicitly be shown to be connected to non-homogeneous anisotropy. For ultrathin films with laterally varying magnetic anisotropy we have shown the existence of the canted state by means of micromagnetic simulations which employ second-order anisotropy constants. The origin of the canting is explicit and solely due to the microstructure. This result is made more transparent by the analytical model which describe the system by means of two macromagnetic moments.

In Ref. [15] it was shown that for films sufficiently thin the role played by the dipolar interaction is negligible. The modulated magnetic configuration is only due to the alternating anisotropy. Such a characteristic may be used in designing magnetic media for perpendicular recording. Pattern with out-of-plane magnetization separated by in-plane regions should store the bit information. Successive parts with out-of-plane anisotropy would be either parallel or anti-parallel magnetized. In both configurations the role played by the dipolar interaction is negligible [23] allowing data storage with high density.

The study presented in this paper has been performed for anisotropic stripe systems made of magnetically flat films. The results of this analysis, however, can be generalized for and applied to real thin film systems. The direction of magnetization for example can be rotated by covering magnetic films with a different material [24]. If the coverage is partially (submonolayer) a locally varying anisotropy is created with lateral dimensions determined by the size of the adlayer islands. Similar microscopic modulations of anisotropy can appear in magnetic thin films that exhibit a thickness-dependent spin reorientation transition. In case of ideal growth, i.e. layer-by-layer, the film thickness varies locally by increments of 1 ML and island are formed. Again this can cause the local variations of magnetic anisotropy when anisotropy changes from one to the next completed layer. Our study is a simple approach to model such systems. The simplification of periodic stripes makes the simulation feasible while reality shows more irregular structures. These structures appear on the same length scale we have covered with our model. Hence, we are quite sure that our results are applicable to a whole class of real systems in the field of ultrathin ferromagnetism.

4. Summary

In this work, we have studied the magnetic configurations in anisotropic stripe systems modelled by means of a series of infinitely long stripes with alternating uniaxial anisotropy. States of uniform, canted and alternating magnetization are found as a function of the period of the structure and of the widths of the stripes. In the limit of narrow stripes the system has been modelled with two macromagnetic moments that describe the canting by means of a fourth order anisotropy term due to the microstructure. We have performed a macroscopic analysis of the system by considering the average magnetization of the magnetic states. In this framework we can demonstrate that all the aspects of the spin reorientation transition between states of uniform magnetization can be recovered by the variation of the lateral scale of the stripes. We have found that the rotation of the average magnetization is always continuous and is sharper for a higher density of stripes.

Acknowledgements

The authors acknowledge fruitful discussions with W. Kuch.

References

[1] J. Shen, J. Kirschner, Surf. Sci. 500 (2002) 300.
[2] R.P. Cowburn, A.O. Adeyeye, J.A.C. Bland, Appl. Phys. Lett. 70 (1997) 2309.
[3] C. Chappert, H. Bernas, J. Ferré, V. Kottler, J.-P. Jamet, Y. Chen, E. Cambril, T. Devolder, F. Rousseaux, V. Mathet, H. Launois, Science 280 (1998) 1919;
B.D. Terris, L. Folks, D. Weller, J.E.E. Baglin, A.J. Kellock, H. Rothuizen, P. Vettiger, Appl. Phys. Lett. 75 (1999) 403.
[4] S.P. Li, W.S. Lew, J.A.C. Bland, L. Lopez-Diaz, C.A.F. Vaz, M. Natali, Y. Chen, Phys. Rev. Lett. 88 (2002) 087202.
[5] M. Scheinfein, The simulations are performed with LLG *Micromagnetic Simulator*^{TM} (see http://llgmicro.home.mindspring.com).
[6] See for instance, A. Aharoni, Introduction to the Theory of Ferromagnetism, Oxford University Press, Oxford, 1996.
[7] J. Kohlhepp, U. Gradmann, J. Magn. Magn. Mater. 139 (1995) 347.
[8] H.J. Elmers, J. Magn. Magn. Mater. 185 (1998) 274.
[9] A. Hubert, R. Schäfer, Magnetic Domains, Springer, Berlin, 1998.
[10] D.L. Mills, Phys. Rev. B 39 (1989) 12306.
[11] L. Udvardi, R. Király, L. Szunyogh, F. Denat, M.B. Taylor, B.L. Györffy, B. Újfalussy, C. Uiberacker, J. Magn. Magn. Mater. 183 (1998) 283.
[12] A. Thiaville, A. Fert, J. Magn. Magn. Mater. 113 (1992) 161.
[13] B. Dieny, A. Vedyayev, Europhys. Lett. 25 (1994) 723;
B. Heinrich, T. Monchesky, R. Urban, J. Magn. Magn. Mater. 236 (2001) 339.
[14] J.C. Slonczewski, Phys. Rev. Lett. 67 (1991) 3172.
[15] F. Porrati, W. Wulfhekel, J. Kirschner, J. Magn. Magn. Mater. 270 (2004) 22.
[16] M.A. Torija, J.P. Pierce, J. Shen, Phys. Rev. B 63 (2001) 092404.
[17] S.D. Bader, J. Magn. Magn. Mater. 100 (1991) 440.
[18] Z.Q. Qiu, J. Pearson, S.D. Bader, Phys. Rev. Lett. 70 (1993) 1006.
[19] E.Y. Vedmedenko, H.P. Oepen, A. Ghazali, J.-C.S. Lévy, J. Kirschner, Phys. Rev. Lett. 84 (2000) 5884.
[20] N.D. Mermin, H. Wagner, Phys. Rev. Lett. 17 (1996) 1133.
[21] See for instance, D.P. Pappas, C.R. Brundle, H. Hopster, Phys. Rev. B 45 (1992) 8169;
S. Hope, E. Gu, B. Choi, J.A.C. Bland, Phys. Rev. Lett. 80 (1998) 1750.
[22] H. Fritzsche, J. Kohlhepp, H.J. Elmers, U. Gradmann, Phys. Rev. B 49 (1994) 15665;
Y. Millev, J. Kirschner, Phys. Rev. B 54 (1996) 4137.
[23] F. Porrati, Ph. D. Thesis, University of Halle-Wittemberg, 2002.
[24] J. Lee, G. Lauhoff, J.A.C. Bland, Phys. Rev. B 56 (1997) R5728;
J. Shen, A.K. Swan, J.F. Wendelken, Appl. Phys. Lett. 75 (1999) 2987.